Fuzzy Multi-class Statistical Modeling for Efficient Total Lesion Metabolic Activity Estimation from Realistic PET Images

Jose George[1,2,3], Kathleen Vunckx[1,4], Elke Van de Casteele[1,2,3], Sabine Tejpar[5], Christophe M. Deroose[4], Johan Nuyts[1,4], Dirk Loeckx[1,3,6], and Paul Suetens[1,2,3]

[1] Medical Imaging Research Center, UZ Leuven, Belgium
[2] IBBT-KU Leuven Future Health Department, Belgium
[3] Medical Image Computing (ESAT/PSI/MIC)
[4] Nuclear Medicine
[5] Gastroenterology
[3,4,5] KU, Leuven, Belgium
[6] icoMetrix NV, Leuven, Belgium

Abstract. ^{18}F-fluorodeoxyglucose (FDG) positron emission tomography (PET) has become the de facto standard for current clinical therapy follow up evaluations. In pursuit of robust biomarkers for predicting early therapy response, an efficient marker quantification procedure is certainly a necessity. Among various PET derived markers, the clinical investigations indicated that the total lesion metabolic activity (TLA) of a tumor lesion has a good prognostic value in several longitudinal studies. We utilize a fuzzy multi-class modeling using a stochastic expectation maximization (SEM) algorithm to fit a finite mixture model (FMM) to the PET image. We then propose a direct estimation formula for TLA and SUV_{mean} from this multi-class statistical model. In order to evaluate our proposition, a realistic liver lesion is simulated and reconstructed. All results were evaluated with reference to the ground truth knowledge. Our experimental study conveys that the proposed method is robust enough to handle background heterogeneities in realistic scenarios.

Keywords: ^{18}F-FDG PET, SEM, FMM, TLA, fuzzy partial volume modeling, convex combination of random variables.

1 Introduction

^{18}F-FDG PET has become the de facto standard in current clinical therapy follow up evaluations. PET can record the metabolic response of several trillions of cells in the human body by the use of radiotracers such as ^{18}F-FDG. The tumor lesion, being more metabolically active, shows a higher tracer uptake in the PET scan, thereby enabling quantification of metabolic activity information in contrast to anatomic imaging modalities like magnetic resonance imaging (MRI), computed tomography (CT), etc. Due to its ability to visualize the functional

N. Ayache et al. (Eds.): MICCAI 2012, Part I, LNCS 7510, pp. 107–114, 2012.

information in the metabolic change, PET has been widely used in therapy response evaluations. PET images are typically normalized for injected dose and patient weight to a scale known as the standardized uptake value (SUV) in g/mL. Several PET derived markers [3, 7, 12] have been used in the literature for the longitudinal evaluation of tumor proliferation. $\mathrm{SUV}_{\max}$ (maximum lesion activity uptake), $\mathrm{SUV}_{\mathrm{mean}}$ (average lesion activity uptake), $\mathrm{SUV}_{\mathrm{peak}}$ (activity uptake in $1cc$ spherical region of interest (ROI) around the $\mathrm{SUV}_{\max}$) [12], TLV (total lesion volume) and TLA (total lesion activity uptake) or TLG (total lesion glycolysis), in the context of ^{18}F-FDG PET, are some of them. However, TLA was found to be clinically relevant in [3, 7]. TLA calculation typically involves tumor delineation, to find TLV, followed by the quantification $\mathrm{TLA} = \mathrm{SUV}_{\mathrm{mean}} \times \mathrm{TLV}$.

The aforementioned functional markers computed from the PET image are corrupted by partial volume effects and acquisition blur. Nonetheless, we recently proposed a direct statistical estimation method, statistical lesion activity computation (SLAC), in [6] for computing TLA, in the presence of blur. SLAC only incorporated a fuzzy two class model to fit a Gaussian mixture of tumor, background and its combinations. However, in realistic scenarios, due to the presence of background heterogeneities, such a model may not be sufficient. In this paper, this direct estimation approach is extended to a fuzzy multi-class model to handle more realistic scenarios. A 3-class fuzzy model to handle heterogeneous tumors was introduced in [8]. Nevertheless, this model ignored the possibility of fuzzy mixing all 3 classes in the model. The main contributions of this paper include a fuzzy multi-class statistical modeling of the PET data with fuzzy mixing of all 'hard' classes involved in the model (in order to handle lesion as well as background heterogeneities) along with a direct estimation formula for TLA and $\mathrm{SUV}_{\mathrm{mean}}$ from the statistical model parameters.

2 Materials and Methods

2.1 Fuzzy Multi-class Modeling

Let the observed PET image and the hidden statistical structure be realizations $\mathbf{y} = \{y_s\}_{s\in\mathcal{S}}$ and $\mathbf{x} = \{x_s\}_{s\in\mathcal{S}}$ of the random fields $\mathcal{Y} = \{\mathcal{Y}_s\}_{s\in\mathcal{S}}$ and $\mathcal{X} = \{\mathcal{X}_s\}_{s\in\mathcal{S}}$ respectively, where $\mathcal{S} = \{1, \ldots, N\}$ is the set of voxels. The unsupervised learning problem consists of estimating the unknown model parameters and the hidden $\mathcal{X}$ from the observed noisy version of $\mathcal{X}$ in $\mathcal{Y}$. In the fuzzy multi-class modeling, each voxel s is associated with a $\mathcal{K}$-dimensional vector $\boldsymbol{\epsilon}_s = [\epsilon_{ks}]_{1\le k\le\mathcal{K}}$ denoting % allocation of each of the $\mathcal{K}$ 'hard' classes. E.g., in the case of a liver lesion falling close to the liver boundary, $\mathcal{K}$ could be 3 due to the contributions from the lesion itself, liver background and normal background. While the statistical part models the uncertainty in the classification, the fuzzy part models the imprecision in voxel membership. Now $\mathcal{X}_s$ in the model takes its value from $\boldsymbol{\epsilon} = [\epsilon_k]_{1\le k\le\mathcal{K}}$ with ϵ_k in the closed interval $[0, 1]$ such that $\sum_k \epsilon_k = 1$. This is achieved by simultaneously using Dirac and Lebesgue measures in the fuzzy model. Then the measure will be $\boldsymbol{\nu} = \sum_i \boldsymbol{\zeta}_i + \sum_j \boldsymbol{\mu}_j$, where $\boldsymbol{\zeta}_i$'s are the Dirac measures on

$\mathcal{K}$ 'hard' classes and $\boldsymbol{\mu}_j$ is the Lebesgue measure with elements on the fuzzy interval $[0,1]$ formed by fuzzy mixing $\mathcal{K}$ 'hard' classes.

To find the conditional density of $\mathcal{Y}_s$ given the hidden classification $\mathcal{X}_s$, consider $\mathcal{K}$ independent and identically distributed (iid) random variables, $\{\mathcal{Y}_k\}_{1\leq k\leq \mathcal{K}}$ associated to $\mathcal{K}$ 'hard' classes with densities $f_{\mathcal{Y}_s}(\xi \mid \mathcal{X}_s = \boldsymbol{\delta}_k)$ defining the distributions of $\mathcal{Y}_s$ conditional to $\mathcal{X}_s = \boldsymbol{\delta}_k$ respectively, where the $\mathcal{K}$-dimensional class labels $\boldsymbol{\delta}_k = [\epsilon_j]_{1\leq j\leq \mathcal{K}}$ such that $\epsilon_j = 1$ for $j = k$. Then the partial volume activities can be modeled by convex combinations of these independent random variables as $\mathcal{Y}_s = \sum_k \epsilon_k \mathcal{Y}_k$, for $\mathcal{X}_s = \boldsymbol{\epsilon}$, and $\boldsymbol{\epsilon} = [\epsilon_k]_{1\leq k\leq \mathcal{K}}$ is the $\mathcal{K}$-dimensional fuzzy mixture class with $\epsilon_k \in]0,1[$, $\sum_k \epsilon_k = 1$. Here the $\mathcal{Y}_k$'s and $\mathcal{Y}_s$ model the noise associated with the k^{th} 'hard' class (for e.g., tumor, lesion background, normal background, etc) and the 'fuzzy' partial volume activities (mixture of 'hard' classes) respectively. If $f_{\mathcal{Y}_s}(\xi \mid \mathcal{X}_s = \boldsymbol{\delta}_k)$'s are Gaussian distributed with densities $\mathcal{N}(\mu_k, \sigma_k^2)$, then $\mathcal{Y}_s$ is again Gaussian distributed with density $\mathcal{N}(\mu_{\boldsymbol{\epsilon}}, \sigma_{\boldsymbol{\epsilon}}^2)$ conditional to $\mathcal{X}_s = \boldsymbol{\epsilon}$, $f_{\mathcal{Y}_s}(\xi \mid \mathcal{X}_s = \boldsymbol{\epsilon})$, such that $\mu_{\boldsymbol{\epsilon}} = \sum_k \epsilon_k \mu_k$ and $\sigma_{\boldsymbol{\epsilon}}^2 = \sum_k \epsilon_k^2 \sigma_k^2$.

Given $\mathcal{K}$ 'hard' classes, there are $2^{\mathcal{K}} - 1$ ways of fuzzy mixing the activities, of which $\mathcal{K}$ are purely belonging to 'hard' classes and the remaining $2^{\mathcal{K}} - \mathcal{K} - 1$ are 'fuzzy'. For $\mathcal{K} = 3$, there are 7 possibilities of mixing viz. '001', '010', '011', '100', '101', '110' and '111' of which the 1^{st}, 2^{nd} and 4^{th} represent 'hard' classes ($\mathcal{H}_i$) and the remaining 4 denote 'fuzzy' classes ($\mathcal{F}_j$). Also, for each of the fuzzy mixing possibilities, we can assign infinite combinations for ϵ_k. However, in our investigations, we use a tolerance of 10% for ϵ_k along with an equal weightage class ($\frac{100}{3}\%$), making it a total of $66 + 1$ class labels including 'hard' as well as 'fuzzy' classes for $\mathcal{K} = 3$. Here onwards, 'class' in general denotes those $2^{\mathcal{K}} - 1 = 7$ combinations, where as 'class label' denotes those 67 mixing possibilities in the model.

In our modeling, we assume $\mathcal{X}_s$ to be non stationary and use an adaptive support window to estimate the *a priori* information locally. Let $\mathcal{Z} = \{\mathcal{Z}_s\}_{s\in\mathcal{S}}$ be the learned hidden classification map at a particular iteration, then the local prior is

$$\gamma_{\mathcal{C}}^{(s)} \leftarrow \frac{\sum_{r\in\mathcal{W}_s} \delta(\mathcal{Z}_r, \mathcal{C})}{Card(\mathcal{W}_s)}, \text{ for } \mathcal{C} \in \{\mathcal{H}_i, \mathcal{F}_j\} \tag{1}$$

where $\mathcal{W}_s$ is a $w \times w \times w$ local support window around voxel s, δ is the Kronecker delta function and $Card(\mathcal{W}_s)$ is the cardinality of $\mathcal{W}_s$. That means for $\mathcal{K} = 3$, there will be a $\gamma_{\mathcal{C}}$ for each of the 7 classes $\{\mathcal{H}_i, \mathcal{F}_j\}$. Now, the *a posteriori* distribution of $\mathcal{X}_s$ with respect to $\boldsymbol{\nu}$ given the noisy observation $\mathcal{Y}_s = y_s$ is given by

$$p_{\mathcal{X}_s}^{(s)}(\boldsymbol{\epsilon} \mid y_s) = \frac{\gamma_{\boldsymbol{\epsilon}}^{(s)} f(y_s \mid \boldsymbol{\epsilon})}{\sum_i \gamma_i^{(s)} f(y_s \mid \mathcal{H}_i) + \sum_j \gamma_j^{(s)} f(y_s \mid \mathcal{F}_j)} \tag{2}$$

where $f(y_s \mid \mathcal{F}_j)$ in the denominator are obtained by numerical integration.

The SEM algorithm [2] is used for iteratively estimating the parameters of the model. It is a stochastic version of the EM algorithm [4] making use of stochastic expectation and maximization steps to efficiently model the PET image. In each iteration, $p_{\mathcal{X}_s}^{(s)}(\boldsymbol{\epsilon} \mid y_s)$ are estimated as in (2). This forms the expectation part of the SEM module. At iteration q, $p_{\mathcal{X}_s}^{(s)}(\boldsymbol{\epsilon} \mid y_s)$ are sampled to estimate the intermediate

labels $\mathcal{Z}_s^q$. The maximization part involves the direct estimation of distribution parameters from $\mathcal{Z}_s^q$ and the local adaptive prior computation using (1). The parameters $\{\mu_k, \sigma_k^2\}$ of the density functions $f_{\mathcal{Y}_s}(\xi \,|\, \mathcal{X}_s = \boldsymbol{\delta}_k)$ are updated from the 'hard' classes in $\mathcal{Z}_s^q$. Then fuzzy parameters $\{\mu_{\boldsymbol{\epsilon}}, \sigma_{\boldsymbol{\epsilon}}^2\}$ are computed.

In order to obtain the hidden variable $\mathcal{Z} = \{\mathcal{Z}_s\}_{s\in\mathcal{S}}$, we sample the posterior distribution $p_{\mathcal{X}_s}^{(s)}(\boldsymbol{\epsilon} \,|\, y_s)$ taking values from $\mathcal{C} = \{\mathcal{H}_i, \mathcal{F}_j\}$ and making use of the maximum posterior likelihood (MPL) method [1]. MPL integrates a dual sampling stage as follows. If $p_{\mathcal{X}_s}^{(s)}(\mathcal{H}_i \,|\, y_s)$ and $p_{\mathcal{X}_s}^{(s)}(\mathcal{F}_j \,|\, y_s)$ are the *a posteriori* densities associated with the $\mathcal{K}$ 'hard' classes and $2^{\mathcal{K}} - \mathcal{K} - 1$ 'fuzzy' classes respectively, then the classification rule assigns to each voxel s the label $\boldsymbol{\eta}$ in $\{\mathcal{H}_i, \mathcal{F}_j\}$ which has the maximum *a posteriori* density. i.e. $\mathcal{Z}_s = \arg\max_{\boldsymbol{\eta}\in\{\mathcal{H}_i,\mathcal{F}\}} p_{\mathcal{X}_s}^{(s)}(\boldsymbol{\eta} \mid y_s)$. If $\mathcal{Z}_s \in \mathcal{H}_i$, i.e. when the classifier opts for hard class labels, the decision rule halts. Otherwise, i.e. when $\mathcal{Z}_s \in \mathcal{F}_j$, the classification proceeds to the second stage decision rule given by $\mathcal{Z}_s = \arg\max_{\boldsymbol{\eta}\in\{\boldsymbol{\epsilon}_k\}} p_{\mathcal{X}_s}^{(s)}(\boldsymbol{\eta} \,|\, y_s)$ to sample one of the fuzzy labels $\boldsymbol{\epsilon}_k$ in $\mathcal{F}_j$.

To deal with initialization, we use random starts. In each of these random starts, a fuzzy C-means clustering routine looks for the initial feasible solution consisting of $2^{\mathcal{K}} - 1$ clusters representing 'hard' as well as 'fuzzy' classes. The model parameters are estimated to compute the message length [5]. The one giving the minimum message length is selected to initialize the SEM algorithm. The initial parameters of $\mathcal{N}(\mu_k, \sigma_k^2)$ and $\mathcal{N}(\mu_{\boldsymbol{\epsilon}}, \sigma_{\boldsymbol{\epsilon}}^2)$ are thus obtained. The local adaptive priors are initialized to $(2^{\mathcal{K}} - 1)^{-1}$ for each voxel. The SEM is run for utmost 100 iterations or until the total absolute relative change in the model parameters as well as the prior between consecutive iterations falls below $1e^{-3}$.

2.2 Direct TLA and $\mathrm{SUV}_{\mathrm{mean}}$ Estimation

Once the fuzzy multi-class modeling is complete, the functional markers TLA and $\mathrm{SUV}_{\mathrm{mean}}$ can be directly computed. A statistical direct computation formula to compute TLA for a fuzzy 2-class model is discussed in [6]. Here, we extend this idea to a fuzzy multi-class model. Total lesion activity (TLA) is the integral of metabolic activity over the whole lesion. It represents the weight of the metabolic lesion in gram (g). For a given ROI, starting from the total PET activity (TPA), constituting contributions from the lesion (TLA) and the background activities, we deduce the relationship between TLA and the SEM model parameters. From the observed PET image voxels $\{y_s\}_{s\in\mathcal{S}}$, TPA $:= \sum_{s\in\mathcal{S}} y_s = \sum_{j\in\mathcal{J}} j\, h(j)$, where $\mathcal{S} = \{1, \ldots, N\}$, $h(j)$ is the observed histogram and $\mathcal{J}$ is the set of observed PET activity levels, $y_s \in \mathcal{J}$. In other words, the total activity in $\mathcal{S}$ is the same as the sum of all activity levels j scaled by respective frequencies of occurrence $h(j)$. Based on the fact that normalization of the observed histogram $h(j)$ gives the associated probability mass function $p(j) = P[\mathcal{Y}_s = j]$, without the loss of generality, TPA $:= \sum_{s\in\mathcal{S}} y_s = N \sum_{j\in\mathcal{J}} j\, p(j)$, where N is the number of voxels. Extending it to the continuous domain and integrating the activity over the whole $\mathcal{S}$, the total PET activity, TPA can be related to the density $f_{\mathcal{Y}_s}(\xi)$ defining the distribution of $\mathcal{Y}_s = \xi$ as well as the 1^{st} moment of $\mathcal{Y}_s$, $E(\mathcal{Y}_s)$ from

the Riemann-Stieltjes integral by TPA $:= N \int \xi f_{\mathcal{Y}_s}(\xi) d\xi = N \times E(\mathcal{Y}_s)$. However, the density $f_{\mathcal{Y}_s}(\xi)$ is a finite mixture $\sum_i \alpha_i f_{\mathcal{Y}_s}(\xi \,|\, \boldsymbol{\epsilon}_i)$, where α_i stands for the mixing probabilities $P[\mathcal{X}_s = \boldsymbol{\epsilon}_i]$ for each of the class labels (67 labels for $\mathcal{K} = 3$) after modeling. If $E(\mathcal{Y}_s \,|\, \boldsymbol{\epsilon}_i)$ represents the conditional expectation of $\mathcal{Y}_s$ given $\mathcal{X}_s = \boldsymbol{\epsilon}_i$, then the TPA $:= N \sum_i \alpha_i \int \xi f_{\mathcal{Y}_s}(\xi \,|\, \boldsymbol{\epsilon}_i) d\xi = N \sum_i \alpha_i E(\mathcal{Y}_s \,|\, \boldsymbol{\epsilon}_i)$.

In the fuzzy modeling, $\mathcal{Y}_s$ is a convex combination of *iid* random variables $\mathcal{Y}_k$'s such that $\mathcal{Y}_s = \sum_k \epsilon_k \mathcal{Y}_k$. Then, the conditional expectation of $\mathcal{Y}_s$ given $\mathcal{X}_s = \boldsymbol{\epsilon}_i$ is $E(\mathcal{Y}_s \,|\, \boldsymbol{\epsilon}_i) = \sum_k \epsilon_{ki} E(\mathcal{Y}_k)$, where ϵ_{ki} is the fraction of the k^{th} 'hard' class in the i^{th} class label. applying the linearity property of the expectation operator and the statistical independence between the random variables $\mathcal{Y}_k$'s. Then the total PET activity is modified as TPA $:= N \sum_i \alpha_i \sum_{k \in \mathcal{K}} \epsilon_{ki} E(\mathcal{Y}_k)$. Now, we have an expression for TPA depending only on the 'hard' class model parameters ($E(\mathcal{Y}_k)$). If among the $\mathcal{K}$ 'hard' classes used for modeling the PET image, only $\mathcal{M}$ classes belong to the tumor, then the total lesion activity (TLA) is given by TLA $:= N \sum_i \alpha_i \sum_{k \in \mathcal{M}} \epsilon_{ki} E(\mathcal{Y}_k)$. Let's go back to the previous case of a liver lesion with 3 dominant classes viz. lesion ($\mathcal{Y}_1$), liver background ($\mathcal{Y}_2$) and normal background ($\mathcal{Y}_3$), the TLA $= N \sum_i \alpha_i \epsilon_{1i} E(\mathcal{Y}_1)$, where ϵ_{1i} is the fraction of lesion class in the i^{th} class label used in the modeling. After modeling, the delineation is made from the fuzzy class labels by selecting voxels with 50% or more allocation of the lesion class as belonging to the lesion. The lesion volume, TLV is the voxel count in that delineation. Once TLA and TLV are accurately estimated, the mean activity can be computed by $\text{SUV}_{\text{mean}} = \frac{\text{TLA}}{\text{TLV}}$.

2.3 Simulated Lesions

To evaluate the performance, an NCAT phantom [11] with a hot liver lesion was simulated. Realistic FDG uptake values were assigned to the various organs and tissues of the NCAT phantom. A non spherical tumor ($27.67mL$) was inserted in the liver (see Fig. 1). In the tumor, the activity was set to $18.2kBq/cc$. The activity in the liver, spleen, lungs and body was $6.3kBq/cc$, $5.5kBq/cc$, $0.9kBq/cc$ and $2.5kBq/cc$ respectively. The voxel size used to generate the phantom was $1mm \times 1mm \times 1mm$. 30 $3min$ scans of the NCAT phantom were simulated using a Monte Carlo simulator (PET-SORTEO [10]) which models among others the spatially variant point spread function (PSF) of the ECAT Exact HR+ scanner. Attenuation and scatter were also modeled. During reconstruction of both datasets, the system PSF resolution was recovered by modeling as an isotropic Gaussian with $5mm$ FWHM. The projection data were reconstructed using the maximum likelihood expectation maximization (MLEM) algorithm [9] with ordered subsets. As in clinical routine, 4 iterations over 16 subsets were performed. The reconstruction voxel size was set to $2mm \times 2mm \times 2mm$. The images were post-smoothed with $5mm$ Gaussian FWHM.

3 Experiments and Results

Fig. 1(a) illustrates transverse slices of the liver lesion along with the binary delineation mask (whose integral gives TLV) obtained by 50% threshold as dis-

cussed in Section 2.2, as well as the lesion falling inside the delineation (commonly integrated for TLA). The liver lesion under study has voxels belonging to the lesion, liver background as well as normal background. So, we model fuzzy multi-class SEM with $\mathcal{K} = 3$ consisting of 67 class labels (see Section 2.1) and $w = 3$. Fig. 1(b) depicts respective transverse slices of images reconstructed from 30 different noise realizations. Fig. 1(c) shows the % allocation of each of the 3 'hard' classes in each voxel location. Fig. 1(d) plots the histogram modeled with 3 'hard' classes and its 'fuzzy' mixtures. Table 1 lists the SUV_{mean} as well

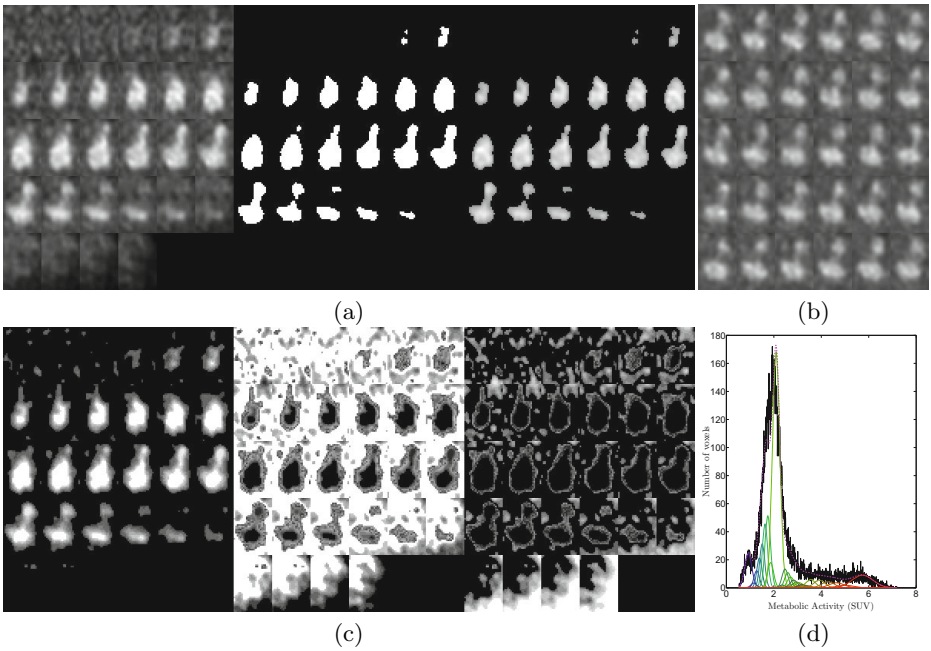

Fig. 1. (a)-Transverse slices of the simulated liver lesion (left), the delineated mask estimated from the model (middle) and the delineated lesion (right) from which TLA is commonly estimated. (b)-Respective slices of the MLEM reconstructed PET images from 30 noise realizations. (c)-Slices showing the percentage allocation of each of the 3 classes viz. the tumor class (left), the liver background class (middle) and the normal background class (right), used in the model. (d)-Actual histogram (in black) modeled as a finite mixture of 3 hard classes (the tumor class in red, the liver background in green and the normal background in blue shade) and a mixture of fuzzy classes (in a combination of red, green and blue shades) representing partial volume voxels; TLA being contributed from the tumor class and the fuzzy classes.

as the TLA obtained using our direct estimation method (*dir*) and computation from delineation (*deli*). In the first case, TLA^{dir} is directly computed as discussed in Section 2.2. Once the delineation is achieved, TLV is computed from it. Then $\text{SUV}_{\text{mean}}{}^{dir} = \frac{\text{TLA}^{dir}}{\text{TLV}}$. In the latter case, $\text{SUV}_{\text{mean}}{}^{deli}$ is estimated

as the mean activity in the delineation. Afterwards, TLA^{deli} is estimated as $\text{TLA}^{deli} = \text{SUV}_{\text{mean}}{}^{deli} \times \text{TLV}$. The TLV estimated at (5, 50, 95) percentile were (24.62, 25.74, 26.68) in mL with % error (-11.04, -6.97, -3.58) resp. Actual TLA and SUV_{mean} from the ground truth knowledge is $166.03g$ and $6g/mL$ resp. The median estimates ($\text{TLA}^{dir} = 162.62g$, $\text{SUV}_{\text{mean}}{}^{dir} = 6.33g/mL$) denote that our method provided the best estimate for both of these markers, whereas the delineation-based method yields an underestimation of the tumor uptake.

Table 1. 5, 50 (median) and 95 percentiles of the mean lesion activity (SUV_{mean}) and the total lesion activity (TLA) estimated using delineation-based (*deli*) and direct (*dir*) approaches from 30 noise realizations, with 3-FLAB [8] and proposed approach

Percentile		3-FLAB estimator [8]				Proposed multi-class estimator			
		deli		*dir*		*deli*		*dir*	
		Value	(% error)	Value	(% error)	Value	(% error)	Value	(% error)
SUV_{mean} (g/mL)	5	4.98	(−17.0%)	6.28	(4.7%)	4.86	(−19.0%)	6.16	(2.6%)
	50	**5.08**	**(-15.4%)**	**6.43**	**(7.1%)**	**4.96**	**(-17.2%)**	**6.33**	**(5.5%)**
	95	5.39	(−10.2%)	8.03	(33.8%)	5.06	(−15.7%)	6.48	(8.1%)
TLA (g)	5	92.47	(−44.3%)	137.71	(−17.1%)	123.53	(−25.6%)	157.39	(−5.2%)
	50	**120.19**	**(-27.6%)**	**152.19**	**(-8.3%)**	**127.77**	**(-23.0%)**	**162.62**	**(-2.1%)**
	95	125.38	(−24.5%)	157.83	(−4.9%)	131.40	(−20.9%)	168.08	(1.2%)

4 Discussion and Conclusion

The experimental studies done with 30 noise realizations of a realistic liver lesion showed again that the current trend of estimating TLA and SUV_{mean} from the delineation lead to underestimation in those PET derived markers. Moreover this underestimation is more pronounced for smaller lesions due to the influence of blur [6] and hence the quantification of these markers for longitudinal lesion evolution studies could be heavily compromised. At this point, our direct computation approach is beneficial. To our best knowledge, there are only few methods developed taking into consideration the need to estimate actual metabolic activity. Moreover, due to the limitation imposed by the PET acquisition system, any approach to delineate the actual tumor lesion will potentially end up underestimating the actual activity. This is in fact substantiated in the relative % errors. The proposed fuzzy multi-class SEM model is computationally fast and relatively robust to initialization compared to the conventional EM algorithm. Basic EM requires better initialization and more iterations to reach convergence. However, SEM achieves that with less iterations. Moreover due to direct parameter estimation, SEM is less computationally intensive. The advantages with fuzzy modeling is that it takes into account the spatially varying resolution automatically within the model. On the contrary, typical partial volume correction schemes assume that the PSF is Gaussian, which is not always the case. We put a tolerance of 10% allocation so that this spatial variability is aptly modeled irrespective of the noise realizations. To a good extent, this is handled as

indicated by the 90% confidence interval (see Table 1). By providing multiple classes in the model, heterogeneous lesion as well as heterogeneous background can be efficiently modeled. The future work includes modeling with other probability distributions, analyzing clinical PET images, application to heterogeneous tumors and robustness study for varying reconstruction parameters.

Acknowledgments. The authors gratefully acknowledge the financial support by KU Leuven's Concerted Research Action GOA/11/006, IWT - TBM project 070717 and Research Foundation - Flanders (FWO).

References

1. Caillol, H., Pieczynski, W., Hillion, A.: Estimation of fuzzy Gaussian mixture and unsupervised statistical image segmentation. IEEE Trans. Image Process. 6(3), 425–440 (1997)
2. Celeux, G., Diebolt, J.: L'algorithme SEM: Un algorithme d'apprentissage probabiliste pour la reconnaissance de mélanges de densités. Revue de Statistique Appliquée 34(2), 35–52 (1986)
3. Costelloe, C.M., Macapinlac, H.A., Madewell, J.E., Fitzgerald, N.E., Mawlawi, O.R., Rohren, E.M., Raymond, A.K., Lewis, V.O., Anderson, P.M., Bassett Jr., R.L., Harrell, R.K., Marom, E.M.: ^{18}F-FDG PET/CT as an indicator of progression-free and overall survival in osteosarcoma. J. Nucl. Med. 50(3), 340–347 (2009)
4. Dempster, A.P., Laird, N.M., Jain, D.B.: Maximum likelihood from incomplete data via the EM algorithm. J. Roy. Stat. Soc. B Stat. Meth. 39(1), 1–38 (1977)
5. Figueiredo, M.A.T., Jain, A.K.: Unsupervised learning of finite mixture models. IEEE Trans. Pattern Anal. Mach. Intell. 24(3), 381–396 (2002)
6. George, J., Vunckx, K., Tejpar, S., Deroose, C.M., Nuyts, J., Loeckx, D., Suetens, P.: Fuzzy Statistical Unsupervised Learning Based Total Lesion Metabolic Activity Estimation in Positron Emission Tomography Images. In: Suzuki, K., Wang, F., Shen, D., Yan, P. (eds.) MLMI 2011. LNCS, vol. 7009, pp. 233–240. Springer, Heidelberg (2011)
7. Hatt, M., Le Rest, C.C., Aboagye, E.O., Kenny, L.M., Rosso, L., Turkheimer, F.E., Albarghach, N.M., Metges, J.P., Pradier, O., Visvikis, D.: Reproducibility of ^{18}F-FDG and 3'-Deoxy-3'-^{18}F-Fluorothymidine PET tumor volume measurements. J. Nucl. Med. 51(9), 1368–1376 (2010)
8. Hatt, M., Le Rest, C.C., Descourt, P., Dekker, A., Ruysscher, D.D., Oellers, M., Lambin, P., Pradier, O., Visvikis, D.: Accurate automatic delineation of heterogeneous functional volumes in positron emission tomography for oncology applications. Int. J. Radiation Oncology 77(1), 301–308 (2010)
9. Hudson, H.M., Larkin, R.S.: Accelerated image reconstruction using ordered subsets of projection data. IEEE Trans. Med. Imag. 13(4), 601–609 (1994)
10. Reilhac, A., Lartizien, C., Costes, N., Sans, S., Comtat, C., Gunn, R.N., Evans, A.C.: PET-SORTEO: A Monte Carlo-based simulator with high count rate capabilities. IEEE Trans. Nucl. Sci. 51(1), 46–52 (2004)
11. Segars, W.P.: Development of a new dynamic NURBS-based cardiac-torso (NCAT) phantom. PhD Dissertation, The University of North Carolina (2001)
12. Wahl, R.L., Jacene, H., Kasamon, Y., Lodge, M.A.: From RECIST to PERCIST: evolving considerations for PET response criteria in solid tumors. J. Nucl. Med. 50(suppl. 1), 122S–150S (2009)